

Multiwavelength detection of an ongoing FUOr-type outburst on a low-mass YSO

Zhen Guo¹,^{1,2,3,4}★ P. W. Lucas¹,⁴ R. G. Kurtev^{1,5} J. Borissova¹,^{1,5} Vardan Elbakyan^{6,7} C. Morris¹,⁴ A. Bayo⁸ L. Smith⁹ A. Caratti o Garatti^{10,11} C. Contreras Peña^{12,13} D. Minniti^{14,15,16} J. Jose¹⁷ M. Ashraf¹⁷ J. Alonso-García^{5,18} N. Miller¹ and H. D. S. Muthu⁴

¹Instituto de Física y Astronomía, Universidad de Valparaíso, ave. Gran Bretaña, 1111, Casilla 5030, Valparaíso, Chile

²Núcleo Milenio de Formación Planetaria (NPF), ave. Gran Bretaña, 1111, Casilla 5030, Valparaíso, Chile

³Departamento de Física, Universidad Técnica Federico Santa María, Avenida España 1680, Valparaíso, Chile

⁴Centre for Astrophysics Research, University of Hertfordshire, Hatfield AL10 9AB, UK

⁵Millennium Institute of Astrophysics, Nuncio Monseñor Sotero Sanz 100, Of. 104, Providencia, Santiago, Chile

⁶Fakultät für Physik, Universität Duisburg-Essen, Lotharstraße 1, D-47057 Duisburg, Germany

⁷Research Institute of Physics, Southern Federal University, Stachki Ave. 194, Rostov-on-Don 344090, Russia

⁸European Organisation for Astronomical Research in the Southern Hemisphere (ESO), Karl-Schwarzschild-Str 2, 85748 Garching bei München, Germany

⁹Institute of Astronomy, University of Cambridge, Madingley Road, Cambridge, CB3 0HA, UK

¹⁰INAF - Osservatorio Astronomico di Capodimonte, salita Moiariello 16, I-80131, Napoli, Italy

¹¹Dublin Institute for Advanced Studies, School of Cosmic Physics, Astronomy and Astrophysics Section, 31 Fitzwilliam Place, Dublin 2, Ireland

¹²Department of Physics and Astronomy, Seoul National University, 1 Gwanak-ro, Gwanak-gu, Seoul 08826, Republic of Korea

¹³Research Institute of Basic Sciences, Seoul National University, Seoul 08826, Republic of Korea

¹⁴Departamento de Ciencias Físicas, Universidad Andres Bello, Republica 220, 8320000 Santiago, Chile

¹⁵Vatican Observatory, V00120 Vatican City State, Italy

¹⁶Departamento de Física, Universidade Federal de Santa Catarina, Trindade 88040-900, Florianópolis, SC, Brazil

¹⁷Indian Institute of Science Education and Research (IISER) Tirupati, Rami Reddy Nagar, Karakambadi Road, Mangalam (PO), Tirupati 517 507, India

¹⁸Centro de Astronomía (CITEVA), Universidad de Antofagasta, Av. Angamos 601, 02800 Antofagasta, Chile

Accepted 2023 December 20. Received 2023 December 19; in original form 2023 September 30

ABSTRACT

During the pre-main-sequence evolution, Young Stellar Objects (YSOs) assemble most of their mass during the episodic accretion process. The rarely seen FUOr-type events are valuable laboratories to investigate the outbursting nature of YSOs. Here, we present multiwavelength detection of a high-amplitude eruptive source in the young open cluster VdBH 221 with an ongoing outburst, including optical to mid-infrared time series and near-infrared spectra. The initial outburst has an exceptional amplitude of >6.3 mag in *Gaia* and 4.6 mag in K_s , with a peak luminosity up to $16 L_{\odot}$ and a peak mass accretion rate of $1.4 \times 10^{-5} M_{\odot} \text{ yr}^{-1}$. The optical to infrared spectral energy distribution of this object is consistent with a low-mass star ($0.2 M_{\odot}$) with a modest extinction ($A_V < 2$ mag). A 100-d delay between optical and infrared rising stages is detected, suggesting an outside-in origin of the instability. The spectroscopic features of this object reveal a self-luminous accretion disc, very similar to FU Orionis, with a low line-of-sight extinction. Most recently, there has been a gradual increase in brightness throughout the wavelength range, possibly suggesting an enhancement of the mass accretion rate.

Key words: accretion, accretion discs – stars: pre-main sequence – stars: protostar – stars: variables: T Tauri, Herbig Ae/Be – infrared: stars.

1 INTRODUCTION

A FUOr-type event, named after the prototype FU Orionis, displays a prominent outburst in its light curve, usually with an amplitude larger than 5 mag in the optical (see the review from Fischer et al. 2022). These events are rarely detected, as once per 10^4 – 10^5 yr per star, estimated by the total known eruptive samples (Scholz 2012; Hillenbrand & Findeisen 2015; Contreras Peña, Naylor & Morrell

2019, and Contreras Peña submitted 2024). So far, only two dozen such events have been confirmed by photometric and spectroscopic data on young stars. Most FUOr-type outbursts share two common photometric signatures (Hartmann & Kenyon 1996), high amplitude (~ 5 mag in optical) and long duration (tens to nearly one hundred years). These two characteristics distinguish FUOrs from the low-amplitude (up to a few mags) and short time-scale (up to a few years) events, such as EXOr-type outbursts with magnetospheric accretion (Herbig 2007). More recently, the eruptive phenomenon has been observed at all stages and stellar masses in star formation, especially among embedded protostars (Contreras Peña et al. 2017a). Notably,

* E-mail: zhen.guo@uv.cl

most infrared-detected eruptive Young Stellar Objects (YSOs) have intermediate observational features between the classical FUOr and EXOr groups (see Contreras Peña et al. 2017b). Theoretical models have been proposed to trigger episodic accretion bursts on YSOs, including gravitational instabilities (Armitage, Livio & Pringle 2001; Kratter & Lodato 2016), thermal instability (Lodato & Clarke 2004; Clarke et al. 2005), magneto-rotational instabilities (MRI; e.g. Zhu, Hartmann & Gammie 2009b; Elbakyan et al. 2021), disc fragmentation (e.g. Vorobyov & Basu 2015), stellar fly-by (Borchert et al. 2022), and evaporation of gas giant planets (Nayakshin, Owen & Elbakyan 2023).

During the FUOr event, unlike the steady magnetospheric accretion seen on most disc-bearing YSOs, the disc material is directly accreted on to the star by the boundary layer accretion mode (Audard et al. 2014). The mass accretion rate during a solar mass FUOr-type outburst can reach $10^{-4} M_{\odot} \text{ yr}^{-1}$, orders of magnitudes higher than the steady accretion stage. Episodic accretion models predict that most of the stellar mass is accumulated during these outbursts (Hartmann & Kenyon 1996). The released gravitational energy can efficiently heat the inner accretion disc, which becomes self-luminous and outshines the photospheric emission (Zhu et al. 2009a; Liu et al. 2022). The near-infrared (NIR) spectra of FUOrs resemble a bright but cool object, with strong absorption bands mainly from the molecules in the circumstellar disc/envelope. Most FUOrs are confirmed by a combination of eruptive photometric light curves along with their unique spectral features (Connelley & Reipurth 2018; Guo et al. 2021).

The eruptive behaviours of FUOrs across different wavelength ranges can provide clues on the origin of the triggering instability (Vorobyov et al. 2021). For instance, Gaia 17bpi had a pre-outburst in the mid-infrared, 500 d before the optical outburst (Hillenbrand et al. 2018), indicating an outside-in propagation of the MRI originated at ~ 1 AU (Cleaver, Hartmann & Bae 2023). In contrast, slow-rising outbursts in both optical and infrared bands are explained by inside-out propagating instabilities (e.g. Lin, Papaloizou & Faulkner 1985). Theoretical models predict months-long delays in the mid-IR light curves when the outburst is triggered by thermal instabilities initiated at several stellar radii from the star (Nayakshin & Elbakyan 2023). The fading stage of FUOrs contains information about the cooling efficiency of the viscous heated accretion disc. The prototypes of FUOrs have remained bright for decades, though fading at quite different rates (Hartmann & Kenyon 1996), but some recently discovered bona fide FUOrs have a rapid fading stage, which has blurred the initial classification of FUOrs. Previous studies preferred the enhancement of line-of-sight extinction as the explanation of the post-outburst rapid decays (Kopatskaya, Kolotilov & Arkharov 2013; Hackstein et al. 2015). However, analytical disc models suggest that the rapid cooling of the accretion disc can result in such decay in the brightness (Szabó et al. 2021; Carvalho et al. 2023).

Lucas et al. 2024 (hereafter LSG24) discovered 222 high-amplitude objects ($\Delta K_s > 4$ mag) from the decade-long Vista Variables in the Via Lactea survey (VVV; Minniti et al. 2010; Saito et al. 2012; Minniti 2016). In this work, we present multiwavelength light curves and spectra of an ongoing outbursting YSO (L222_78, RA: 17:18:19.65 Dec: $-32:22:53.11$) from the catalogue provided by LSG24. This target is associated with the young open cluster VdBH 221 (Cantat-Gaudin & Anders 2020). The outburst on this object reached 6.3 mag in *Gaia* *G*-band, followed by a short fading stage and a unique recent brightening across the wavelength spectrum.

2 OBSERVATION AND DATA REDUCTION

The eruptive behaviour of L222_78 was originally discovered in LSG24 using the K_s time series from the VVV Infrared Astrometric Catalogue (VIRAC2 β ; Smith et al. 2018, and in preparation). The VIRAC2 β catalogue provides PSF (point spread function) photometry of dozens of K_s detections (from 2010 to 2019) and two multicolour (*Z, Y, J, H*) epochs. A few epochs at/after the photometric maximum are saturated in the VVV images, which were corrected by custom-designed aperture photometry in LSG24.

In 2021 and 2022, we obtained single-epoch *J, H, K_s* photometry of this target using the Son OF ISAAC (Infrared Spectrometer And Array Camera) infrared imager on the New Technology Telescope of European Southern Observatory (SOFI, ESO NTT, Moorwood; Cuby & Lidman 1998). We obtained optical to NIR photometry from the SMARTS 1 m telescope in 2022 and the Rapid Eye Mount (REM) telescope in 2023. Two epochs of *r* and *i*-band images are found in the Las Cumbres Observatory science archive (LCO, Brown et al. 2013). Plus, we retrieved *g, r,* and *i*-band images of the *VPHAS+* survey taken by the VLT (Very Large Telescope) Survey Telescope (VST) from the ESO archive (Drew et al. 2014), and broad-band calibrated images from *ATLAS* forced photometry server (Tonry et al. 2018). Custom-designed aperture photometry measurements were applied to extract the brightness (see Guo et al. 2018).

We retrieved optical light curves and astrometry data from *Gaia* DR3 (*Gaia* Collaboration 2016, 2023). Since this object is not included in the *Gaia* Photometric Science Alert, the archived data only includes observations up until circa 2017. The *Gaia* parallax measurement of L222_78 is 0.9209 ± 0.0218 mas, which is equivalent to a distance of 1.08 ± 0.02 kpc.

We obtained mid-infrared photometric data from *ALLWISE* (Wright et al. 2010) and *NEOWISE* (Mainzer et al. 2014) surveys via the NASA/IPAC Infrared Science Archive. Due to the low spatial resolution, L222_78 is blended with a nearby companion ($d = 2.2''$). We performed custom-written PSF photometry on these two sources, using the epoch-binned *unWISE* images (Lang 2014; Meisner, Lang & Schlegel 2017), obtained from the online *WISEVIEW* tool.¹ The PSF functions were generated in each image ($2' \times 2'$) by the DAOPHOT package, using the 30 brightest sources in the field (Stetson 1987). Then, the PSF function is applied to the target and companion with fixed central locations obtained from the VVV survey. Finally, we obtained the best-fitting heights of the PSF functions for both sources using the least χ^2 method. The typical uncertainty around the photometric maximum is 0.1 mag and enhanced to 0.5 mag around the photometric minimum. There was no detection from *Spitzer*.

Two spectra of L222_78 were observed in 2021 and 2023. The XSHOOTER spectra (Vernet et al. 2011) were obtained on the Very Large Telescope on April 16th 2021. We used optical and NIR arms of the XSHOOTER with slit widths of $0.9''$ in the optical and $0.6''$ in the NIR, with exposure times of 210 s and 300 s, respectively. The data was reduced using the pipeline package built on the REFLEX platform (Freudling et al. 2013). We applied the MOLECFIT software to correct the telluric absorption and to generate wavelength solution of 2nd-order polynomial (Kausch et al. 2015; Smette et al. 2015). On May 9th 2023, we obtained NIR spectra from the Folded-port Infra-Red Echelle spectrograph on the Magellan Baade Telescope (Simcoe et al. 2013). The spectra are composed of four 90 s exposures in the ABBA mode using the $0.6''$ slit. An A0-type telluric standard

¹<http://byw.tools/wisview>.

is obtained afterwards. We applied the FIREHOSE v2.0 pipeline to reduce the data (Gagne et al. 2015), using similar methods described in Guo et al. (2020).

3 RESULTS

3.1 Photometric features

The optical to infrared lightcurves of L222_78, from 2010 to 2023, are presented in Fig. 1. We divide the entire eruptive event into four stages based on the light-curve morphology: the pre-eruptive pre-outbursting stage, the rising stage, the post-peak decaying stage, and the re-brightening stage. The K_s (VVV and SOFI) and *WISE* photometry are obtained throughout all stages, and the post-eruptive decaying stage is well-covered by *Gaia* light curves. Several sparse multicolour photometry (g , r , i , and *VISTA* filters) are obtained at both pre-outbursting and post-eruptive stages, which are applied to measure the spectral energy distribution (SED) of the target.

The rising stage of the outburst started in Oct 2013 and reached the peak brightness before Feb 2015, captured by the *WISE* and *Gaia* data. In the optical, the outburst has an exceptionally fast eruptive stage, as $\Delta G > 6.3$ mag within 170 d, resembling the behaviour of FU Ori. The first *Gaia* epoch was 338 d after the beginning of the NIR outburst. Nevertheless, a lower limit of the pre-outbursting G magnitude (G_{low}) is estimated by the photometric transformation equation as 20.17 mag², and a higher value is found from the synthetic photometry of the best-fitting photospheric model (see 3.2). The duration of the eruptive stage across different bands will be further addressed by analytical functions in Section 3.3.

After reaching the photometric maximum, the *Gaia* light curves of L222_78 entered a decaying stage, whilst its infrared brightness remained relatively constant. We present the G_{BP} and G_{RP} colour-magnitude diagram in Fig. 1. The optical decay agrees with the extinction law assuming $R_V = 3.1$ and $A_V = 1.0$ mag (Wang & Chen 2019). Based on the *Gaia* light curves, we generated a time-extinction correlation to reconstruct the peak brightness in VVV filters. The variation of extinction is not unusual on FUOrs, which has been referred to as the dust grain condensation when the wind collides with the envelope (see Siwak et al. 2023) or the dust lifted by the outflow during the ejection outburst. Such a dimming event is observed on V1057 Cyg, which faded 2 mag in 3 yr after reaching the peak (Herbig 1977). The post-peak A_V enhancement has also been confirmed in several FUOrs, including V960 Mon and Gaia21btb (Hackstein et al. 2015; Siwak et al. 2023).

A low-amplitude colourless brightening trend is detected in the *ATLAS* light curves (see Fig. 1 and the online supplementary file), which is inconsistent with the extinction law mentioned above. The same rising trend is detected in the mid-infrared, indicating a piling up of warm material in the circumstellar disc, which resembles the behaviour of PGIR 20dci (Hillenbrand et al. 2021). However, in the latter case, there was a secondary outburst a decade after the primary outburst, which has not happened yet on L222_78. Nevertheless, we observe a change in the slope of the NIR continuum spectra, which can be interpreted as variable extinction (see Section 3.4). Therefore, we conclude that the recent rising trend on L222_78 is likely attributed to a mixture of increasing mass accretion rate and clearing of line-of-sight extinction. The enhancement in the mid-infrared brightness also suggests the existence of warm dust in the circumstellar disc.

3.2 SED and bolometric luminosity

We present the pre-outburst and outbursting SEDs of L222_78 using photometric data obtained between 0.5–22 μm . The pre-outbursting SED comprises VVV photometry taken in 2010, the *VPHAS+* i -band in 2013 and *WISE* bands from our PSF photometry. We assume no significant variability ($\Delta m > 0.5$ mag) during the pre-outbursting stage. For the in-outburst (peak) brightness, we adopted *Gaia* and *NEOWISE* detection at/near the photometric maximum. The VVV magnitudes were measured ~ 100 d after the photometric maximum, which was affected by the enhancement of the extinction. Hence, the peak VVV magnitudes were estimated by correcting the extinction estimated from the *Gaia* light curves (see Section 3.1). We then performed a least- χ^2 fitting of the pre-outbursting SED to BT-Settl models (Barber et al. 2006; Allard, Homeier & Freytag 2011; Caffau et al. 2011) using the VOSA tool (Bayo et al. 2008) with a fixed *Gaia* distance (1.08 kpc) and A_V ranging between 0–5 mag.

The pre-outbursting SED fitting result suggests that the progenitor has an effective temperature of 3100 K (1σ confidence: 2769–3373 K) and a bolometric luminosity, $L_{\text{bol}} = 0.16 \pm 0.02 L_{\odot}$. The stellar luminosity is a lower limit as there was barely any photospheric emission having been detected. The star could be heavily embedded and therefore be intrinsically bluer and more massive. The infrared excess can be fit by a single temperature blackbody (550 \pm 25 K), although the fitting around 3.6 μm is poor, suggesting a temperature gradient in the circumstellar disc. From the best-fitting photosphere to the pre-outbursting SED, we compute the synthetic magnitude in G and r during the pre-outbursting stage, as $G_{\text{syn}} = 19.5$ mag and $r_{\text{syn}} = 21.4$ mag. Accurate measurements of the L_{bol} at the outbursting stage rely on the precise estimation of A_V . The post-outbursting spectra suggest very low extinction, with $A_V < 1$ mag (see Section 3.4). Therefore, the outbursting bolometric luminosity is between 9–16 L_{\odot} when assuming A_V ranging between 0–1 mag. Under the assumption that the accretion luminosity (L_{acc}) is roughly equal to the bolometric luminosity during the eruptive stage, we estimated the peak mass accretion rate (\dot{M}_{acc}) is 0.8 to $1.4 \times 10^{-5} M_{\odot} \text{ yr}^{-1}$, by simply applying an approximated correlation, $\dot{M}_{\text{acc}} = L_{\text{acc}} R_*/(GM_*)$, (Gullbring et al. 1998). The peak absolute brightness of this source ($M_G \sim 3$ mag) indicates is considerably fainter than any observed stellar merger ($M_V < -3$ mag; Karambelkar et al. 2023) but not inconsistent with a star-planet merger, such as the candidate event ZTF SLRN-2020 (De et al. 2023). However, such events only last for a few hundred days. In contrast, L222_78 has been in the outbursting phase for nearly a decade, suggesting a larger reservoir of the accreted material (i.e. the young accretion disc).

3.3 Rising time-scale

The rising stage of L222_78 was captured by a broad wavelength range, including an exceptional optical amplitude ($\Delta G > 6.3$ mag) which places it as one of the highest amplitude eruptive events on YSOs. We applied analytical functions to describe the exponential rising stage in G , K_s , and $W2$ using observed and synthetic magnitudes. We adopted the two-step formalism originally designed by LSG24,

$$t < t_{1/2} : \quad m(t) = m_q - \frac{m_q - m_p}{1 + e^{-(t-t_{1/2})/\tau}}, \quad (1)$$

$$t \geq t_{1/2} : \quad m(t) = m_q - (m_q - m_p)(0.5 + 0.5(t - t_{1/2})/2\tau), \quad (2)$$

where $t_{1/2}$ is the time when the brightness is enhanced by half of the amplitude and τ is a time-scale parameter. Additionally, m_q

²According to the *Gaia* EDR3 document, $G - g < -(g - i) + 1.0$.

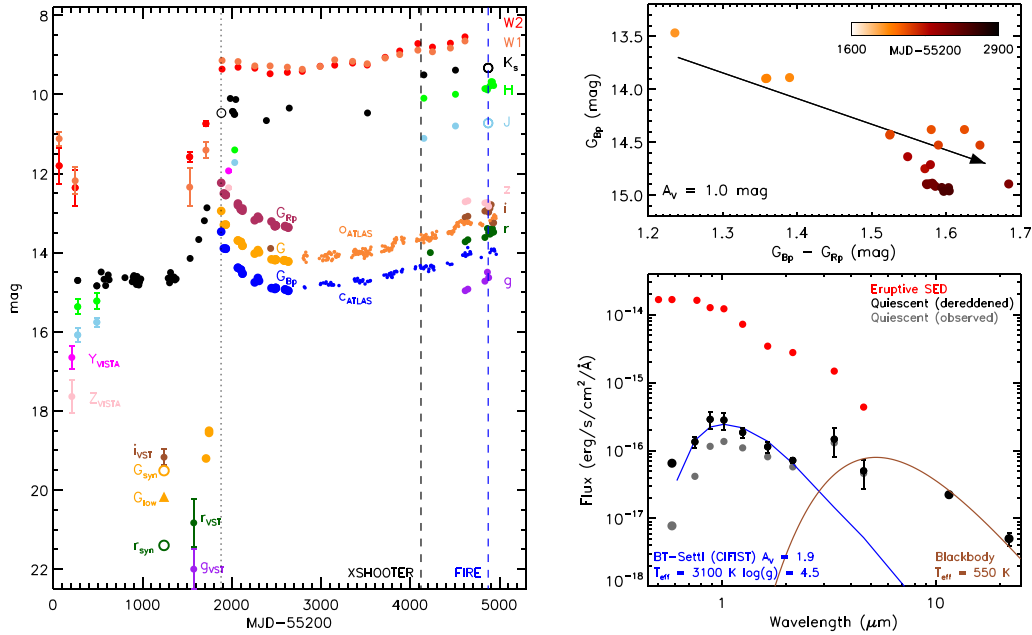


Figure 1. *Left:* multiwavelength light curves of L222_78, colour coded by photometric bands. Error bars less than 0.1 mag are not shown. Open symbols are synthetic magnitudes computed from the SED best-fitting atmospheric model and spectra. Vertical dashed lines mark the observation dates of two spectral epochs. The ending point of the rising stage is shown by the dotted line (around MJD 57080/2015-02-27). *Upper Right:* *Gaia* colour-magnitude diagram with an extinction vector ($A_V = 1.0$ mag). The data points are colour-coded by the observation time. *Lower Right:* The pre-outbursting (grey), dereddened (black), and eruptive (red) SEDs. A BT-Settl model (blue) is fit to the pre-outbursting SED and a blackbody model (brown) is fit to the IR excess beyond 2 μm .

and m_p are the pre-outbursting and peak magnitudes obtained from the time series which are treated as constants in our fitting. As designed, the photometric maximum (m_p) is reached at $t_{1/2} + 2\tau$, where the rising stage ends. This formalism reflects the classical rising morphology of most YSO outbursts in LSG24, composed of a slow-rising stage at the beginning that gradually accelerates before reaching a constant rate of brightening until reaching the photometric maximum.

Here, we used the photometric maximum captured by *Gaia* and *NEOWISE* near MJD 57083, and the synthetic peak magnitude in K_s (measured from the SED fitting above) as m_p . For m_q , we took the mean magnitude in K_s and $W2$ before MJD 56400, plus the G_{syn} and G_{lim} estimated in previous sections. We applied the χ^2 minimization method on two free parameters ($t_{1/2}$ and τ) with grid sizes of 1 d. The light curves, best-fitting analytical curves, and fitting parameters are presented in Fig. 2. In most cases, the analytical functions fit the data well, except in K_s where the brightness increased slightly faster than the model in the first 200 d.

To compare the rising stages across different wavelengths, we present the normalized rising curves on the bottom right panel of Fig. 2. We found that the choice of pre-outbursting magnitude, either G_{syn} or G_{lim} , does not significantly affect the fitting results in G . The infrared bands ($W2$ and K_s) started rising earlier and reached the $t_{1/2}$ point 60–100 d quicker than the G -band. The curve in G is much steeper (smaller τ) than the infrared, indicating a faster-rising nature in optical, with 170 d in the rising stage. However, this rising time-scale is much longer than is typically the case in stellar mergers, though there are exceptions (Karambelkar et al. 2023, and references therein), and they often fade quickly afterwards (Tylenda et al. 2011). The delay between the optical and infrared rising light curves agrees with the phenomenon predicted by the outside-in

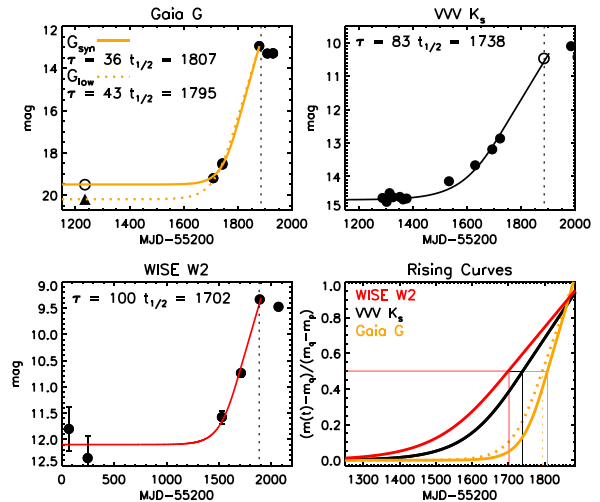


Figure 2. Rising light curves and analytical rising functions of L222_78. Synthetic brightness (open circles) and lower limit (triangle) in G are presented. The normalized curves are shown in the bottom right with $t_{1/2}$ marked out. The ending of the raising stage is marked by the dashed vertical lines.

propagation of the FUOr outburst (Cleaver et al. 2023). However, the time delay observed on L222_78 is five times shorter than the delays on *Gaia*17bpi and *Gaia*18dvy (about 500 d; Hillenbrand et al. 2018; Szegedi-Elek et al. 2020). Theoretically, the duration of the delay is consistent with the viscous time-scale of the disc, proportional to the square root of the disc mass, which should be similar among

low-mass YSOs. We will discuss the triggering mechanisms in Section 4.

3.4 Spectroscopic features

During a FUOr-type event, the viscously heated inner accretion disc becomes more luminous than the stellar photosphere, hence a cool but bright spectrum is observed in the infrared, and a hotter G/K-type spectrum in the optical. The optical spectrum of L222_78, obtained after the outburst, is presented in the upper panel of Fig. 3. It contains a forest of absorption features that are very similar to other FUOrs (e.g. Hillenbrand et al. 2023), rather than other eruptive events, such as stellar mergers. The blueshifted H α absorption feature and the P Cygni profiles on Ca II indicate a wind launched during the outburst, a characteristic property of FUOrs (see Hillenbrand et al. 2019; Szabó et al. 2021). We detected a broad Li λ 6708Å absorption line ($EW = 0.57 \pm 0.08$ Å, integrated between 6707 to 6713Å), as a common indicator of a young age (e.g. Bayo et al. 2011; Campbell-White et al. 2023), and well matches the 1–2 Myr age estimation (Class II YSO). Additionally, the Na I lines exhibit broad spectral profiles (full width at half-maximum = 86 km s⁻¹), which indicates a possible disc origination and is consistent with the Keplerian velocity at the 0.02 AU radius of a 0.2 M $_{\odot}$ star. Such a bright gas disc has been predicted by theoretical models (Liu et al. 2022) and has been observed on several young eruptive YSOs that were classified as bona fide FUOrs (Park et al. 2020; Szabó et al. 2022). More detailed spectral features are presented in the online supplementary material.

In the infrared, the unique spectral absorption features of FUOrs often resemble cool stars, such as the water vapour absorption arising from a low-gravity disc atmosphere, H I lines, deep He I absorption at 1.08 μ m (typically associated with strong non-collimated winds), CO bandheads at 2.3 μ m, and many other molecular bands (e.g. VO, TiO; Connelley & Reipurth 2018). Notably, no jet/outflow feature (e.g. [Fe II], H $_2$) is detected. In the lower panel of Fig. 3, we compared the dereddened XSHOOTER spectrum of L222_78 with the spectrum of FU Ori published in Connelley & Reipurth (2018). Both spectra exhibit similar features, although He I absorption is much deeper on L222_78. Following the method applied in Connelley & Reipurth (2018), we estimated the line-of-sight extinction of L222_78 by aligning the H-bandpass continuum with FU Ori, as $A_V = 1.0$ mag. By fitting the CO overtone models to the spectrum beyond 2.3 μ m (see details in Contreras Peña et al. 2017b), we derived the radial velocity of the CO absorption feature as -10 ± 5 km s⁻¹, with an effective temperature of $T_{\text{eff}} = 3500 \pm 500$ K.

Spectroscopic variability is detected between the two epochs and interpreted as variable extinction, see a comparison between the two NIR spectra of L222_78 in the online supplementary file. The difference in the spectral slope between the two epochs can be well fitted by slightly modifying the line-of-sight extinction by $A_V = 1.2$ mag. We measured $A_H = 0.16$ mag between the two spectra, which is smaller than the contemporary photometric variability ($\Delta H = 0.24$ mag). The dereddened spectra of L222_78 show great similarity to the dereddened IRTF spectra of FU Ori, assuming $A_V = 2.1$ mag (Liu et al. 2022). The low extinction estimated from our NIR spectra suggests that L222_78 should have recovered from the post-peak extinction event. Compared with the estimated extinction in the pre-outburst SED ($A_V = 1.9$ mag), it is quite reasonable to assume that the outburst has cleared out the immediate line-of-sight extinction, also contributing to the high optical amplitudes.

3.5 L222_78 as a young stellar object

We provide the following evidence to support a pre-MS classification of L222_78. First, this target has been classified as a member of a young open cluster VdBH 221 according to the *Gaia* data with a membership probability of unity (see the catalogue in Dias et al. 2021, and fig. C1). We also find a few cold gas clumps located in the vicinity of this target, such as PGCC G354.05+02.95 (10' away, Planck Collaboration 2016), although L222_78 is not directly projected into this cold clump. Second, the pre-outburst SED models suggest $T_{\text{eff}} \sim 3100$ K and $L_{\text{bol}} \sim 0.16 L_{\odot}$, placing this target in the zone of pre-MS stars on the H–R diagram, with an infrared excess. According to evolutionary models (Baraffe et al. 2015), this target is a $\sim 0.2 M_{\odot}$ YSO with an age of 1–2 Myr and radius of 1.1 R $_{\odot}$. The 1–2 Myr of age is younger than the 10 Myr age of the VdBH 211 cluster (Dias et al. 2021), although multigeneration star formation is common among young clusters. Additionally, the pre-outburst NIR colour indices ($J - H = 0.71$ and $H - K_s = 0.43$) are consistent with the intrinsic colours of Class II YSOs (Meyer, Calvet & Hillenbrand 1997). The infrared spectral index α (Lada 1987, measured from 2 to 24 μ m), suggests L222_78 is a Class II YSO ($\alpha = -1.1$). The optical spectrum of L222_78 is very similar to previously detected FUOrs, such as the blue-shifted H α and P Cygni profiles on the Ca II absorption lines. Finally, we detected the Li absorption line, a well-established indicator of a young age (see Section 3.4).

4 DISCUSSION, REMARKS, AND SUMMARY

This study presents an ongoing eruptive object located in the VdBH 221 open cluster, with a 6.3 mag outburst observed in the *Gaia* time series with an optical rising stage of 170 d. A short time delay ($\Delta t_{1/2} = 100$ d) is observed between the infrared and optical rising stages, suggesting an outside-in propagated instability that originated in the circumstellar disc at a radius less than 0.1 AU. Some lower amplitude variations are detected after the photometric maximum, attributed to the gradual changing of line-of-sight extinction and overall mass accretion rate. The prevalence of absorption features in the optical to NIR spectra agrees with the FUOr-type outburst. We conclude that this source is a bona fide FUOr-type object based on the current evidence and the criteria proposed in Connelley & Reipurth (2018). Long-term monitoring is required to determine the full time-scale of this event and to establish a definitive classification.

In the scenario of magneto-rotational activation at the dead zone (Armitage et al. 2001; Elbakyan et al. 2021; Nayakshin & Elbakyan 2023), the burst is thermally triggered when the mid-plane temperature exceeds the critical temperature of ~ 800 K. The disc at this location becomes ionized, and the heatwave propagates inwards from beyond 0.2 AU. However, the predicted time delay is on the scale of 10³ d, much longer than the delay observed on L222_78. Nevertheless, for a short time delay, the instability must originate closer to the star (i.e. 0.07 AU; Liu et al. 2022), which is a small radius for MRI activation. As a reference, such events were predicted to happen in the magnetic field dead zone located around 1 AU for a solar mass star (see Nayakshin & Elbakyan 2023).

Alternatively, an outside-in burst could be introduced by an embedded massive proto-planet, which introduces the thermal instability bursts by opening a gap and piling up material behind its orbit (TIP + EE; Lodato & Clarke 2004; Nayakshin & Elbakyan 2023; Nayakshin et al. 2023). In this scenario, the outburst starts outside the planetary orbit (<0.1 AU) and propagates inwards, creating a

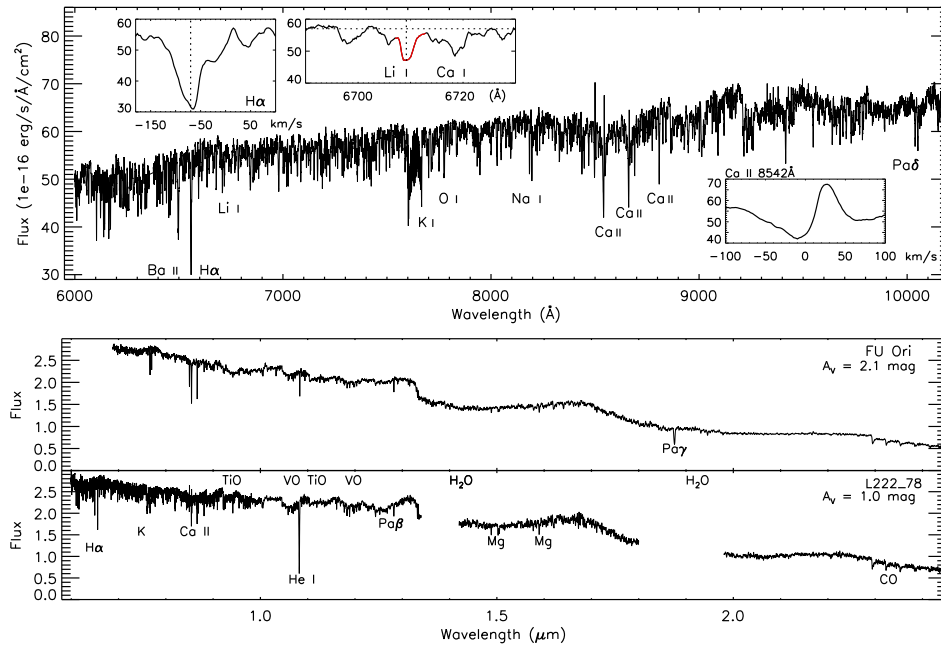


Figure 3. *Upper:* optical spectrum of L222_78, with line profiles of H α , Li I, and Ca II absorption lines. *Lower:* dereddened NIR spectra of FU Ori (InfraRed Telescope Facility; Connelley & Reipurth 2018) and L222_78 (XSHOOTER). Spectral features are marked individually on the plot.

months-long time delay between the optical and infrared bands, consistent with the delay observed on L222.78. The predicted peak mass accretion rate is on the order of $10^{-5} M_{\odot} \text{ yr}^{-1}$, similar to our measurements on L222.78. During the outbursting stage, the temperature of the surrounding proto-planetary material will become higher than the planet’s temperature. As a result, the proto-planet can go through the ‘extreme evaporation’ (EE) phase, during which it is disrupted thermally (Nayakshin et al. 2023).

After the initial outburst, a rise in the visual extinction ($A_V \sim 1$ mag) has been detected by the *Gaia* time series. This change in extinction could be caused by temporary circumstellar dust structures that form subsequent to the outburst, lifted by the strong wind launched from the ejection burst, consequently affecting the optical depth at shorter wavelengths. This extinction event has not changed the overall eruptive phenomenon observed in the *Gaia* light curves ($\Delta G > 6.3$ mag). This is unlike the rapid fading V1647 Ori-type objects, whose 5 mag outburst has completely faded in 1000 d. According to the most recent NIR spectra, the extinction has been cleared out in the past years.

We discover a continuous brightening trend in recent years, from optical (1 mag) to mid-infrared (0.8 mag), which is a novel feature compared to the traditional FUOr-type. This brightening trend can be explained as an increased emission of the system, likely attributed to the eruptive energy heating up the circumstellar disc. Theoretically, a secondary rise is predicted by both the aforementioned TIP + EE and MRI models, attributed to the feeding from the evaporated planetary atmosphere or the change in the mean molecular weight of the gas as Hydrogen is ionized (see details in Nayakshin & Elbakyan 2023).

Using VOSA, we fit a grid of BT-Settl models to the pre-outbursting SED. The synthetic magnitudes derived from the best-fitting model are $G_{\text{syn}} = 19.5$ and $r_{\text{syn}} = 21.4$ mag. Compared with the peak brightness, we find $\Delta G = 6.6$ mag and $\Delta r = 8.6$ mag, ranking L222.78 among the highest amplitude outbursts on YSOs. The

clearing of extinction during the outburst could partially contribute to the optical amplitude. The SED fitting result shows that L222.78 is a low-mass YSO ($0.2 M_{\odot}$) with low extinction ($A_V = 1.9$ mag). The peak mass accretion rate is estimated as up to $1.4 \times 10^{-5} M_{\odot} \text{ yr}^{-1}$, indicating $\sim 40 M_{\oplus}$ have been accreted since the beginning of the outburst. Remarkably, only a few FUOrs were detected within a comparable mass range in the literature, such as V2775 Ori and V346 Nor (Caratti o Garatti et al. 2011; Kóspál et al. 2021). Both sources have relatively heavy and gravitational-unstable circumstellar discs ($M_d > 0.25 M_{*}$), making them good candidates for GI-triggered outbursts. Future sub-mm observations are anticipated to measure the disc mass of L222.78, to unveil the underlying triggering mechanism. Currently, with a low foreground extinction, L222.78 (despite its distance) is an excellent target for high-resolution follow-up observation, to enable studies on the outbursting behaviours of FUOrs.

ACKNOWLEDGEMENTS

We thank Prof M. Connelley for sharing the spectrum of FU Orionis originally taken by IRTF. We appreciate the instructive comments and suggestions from the anonymous referee. ZG is supported by the ANIDFONDECYT Postdoctoral programme no. 3220029. ZG acknowledges support by ANID, – Millennium Science Initiative Program – NCN19.171. ZG, PWL, and CJM acknowledge support by STFC Consolidated grants ST/R00905/1, ST/M001008/1, and ST/J001333/1 and the STFC PATT-linked grant ST/L001403/1. This work has made use of the University of Hertfordshire’s high-performance computing facility (<http://uhhpc.herts.ac.uk>).

JAG, JB, and RK thank the support from ANID’s Millennium Science Initiative ICN12.009, awarded to the Millennium Institute of Astrophysics (MAS). JAG acknowledges support also from Fondecyt Regular 1201490. ACG acknowledges support from INAF-GOG ‘NAOMY: NIR-dark Accretion Outbursts in Massive Young stellar

objects' and PRIN 2022 20228JPA3A – PATH. VE acknowledges the support of the Ministry of Science and Higher Education of the Russian Federation (State assignment in the field of scientific activity 2023, GZ0110/23-10-IF). DM gratefully acknowledges support from the ANIDBASAL projects ACE210002 and FB210003, from Fondecyt project no. 1220724, and from CNPq Brasil project 350104/2022-0.

We gratefully acknowledge data from the ESO Public Survey programme ID 179.B-2002 taken with the VISTA telescope, and products from the Cambridge Astronomical Survey Unit (CASU). This work contains data from ESO programs 105.20CJ and 109.233U, using SOFI on NTT and XSHOOTER on VLT. This research has made use of the NASA/IPAC Infrared Science Archive, which is funded by the National Aeronautics and Space Administration and operated by the California Institute of Technology. This work has made use of data from the European Space Agency (ESA) mission *Gaia* (<https://www.cosmos.esa.int/gaia>), processed by the *Gaia* Data Processing and Analysis Consortium (DPAC, <https://www.cosmos.esa.int/web/gaia/dpac/consortium>). Funding for the DPAC has been provided by national institutions, in particular, the institutions participating in the *Gaia* Multilateral Agreement. This paper includes data gathered with the 6.5 m Magellan Telescopes located at Las Campanas Observatory, Chile. We acknowledge the support from the 1.0 m SMART telescope (operated by the SMARTS Consortium). This publication makes use of VOSA, developed under the Spanish Virtual Observatory project supported by the Spanish MICINN through grant AyA2008-02156.

DATA AVAILABILITY

The WISE data underlying this article are publicly available at the IRSA server <https://irsa.ipac.caltech.edu/Missions/wise.html>. The SOFI, VVV, and VST data are publicly available at the ESO archive <http://archive.eso.org/cms.html>. The VIRAC2 β version of the VVV/VVVX light curves has not yet been publicly released but is available on request to the first author. The raw photometric data obtained by REM and SMART are available upon request. The *Gaia* light curves and photometric measurements are published on the ESA website (<https://www.cosmos.esa.int/gaia>). The ATLAS data is available via the webpage of the survey. Reduced spectra are provided at <http://star.herts.ac.uk/~pwl/Lucas/GuoZ/VVVspec/>.

REFERENCES

Allard F., Homeier D., Freytag B., 2011, in Johns-Krull C., Browning M. K., West A. A., eds, ASP Conf. Ser. Vol. 448, 16th Cambridge Workshop on Cool Stars, Stellar Systems, and the Sun. Astron. Soc. Pac., San Francisco, p. 91

Armitage P. J., Livio M., Pringle J. E., 2001, *MNRAS*, 324, 705

Audard M. et al., 2014, in Beuther H., Klessen R. S., Dullemond C. P., Henning T., eds, Protostars and Planets VI, Univ. Arizona Press, Tucson, p. 387

Baraffe I., Homeier D., Allard F., Chabrier G., 2015, *A&A*, 577, A42

Barber R. J., Tennyson J., Harris G. J., Tolchenov R. N., 2006, *MNRAS*, 368, 1087

Bayo A. et al., 2011, *A&A*, 536, A63

Bayo A., Rodrigo C., Barrado Y Navascués D., Solano E., Gutiérrez R., Morales-Calderón M., Allard F., 2008, *A&A*, 492, 277

Borchert E. M. A., Price D. J., Pinte C., Cuello N., 2022, *MNRAS*, 510, L37

Brown T. M. et al., 2013, *PASP*, 125, 1031

Caffau E., Ludwig H.-G., Steffen M., Freytag B., Bonifacio P., 2011, *Sol. Phys.*, 268, 255

Campbell-White J. et al., 2023, *A&A*, 673, A80

Cantat-Gaudin T., Anders F., 2020, *A&A*, 633, A99

Caratti o Garatti A. et al., 2011, *A&A*, 526, L1

Carvalho A. S. et al., 2023, *Apl*, 953, 86

Clarke C., Lodato G., Melnikov S. Y., Ibrahimov M. A., 2005, *MNRAS*, 361, 942

Cleaver J., Hartmann L., Bae J., 2023, *MNRAS*, 523, 5522

Connelley M. S., Reipurth B., 2018, *ApJ*, 861, 145

Contreras Peña C. et al., 2017a, *MNRAS*, 465, 3011

Contreras Peña C. et al., 2017b, *MNRAS*, 465, 3039

Contreras Peña C., Naylor T., Morrell S., 2019, *MNRAS*, 486, 4590

Contreras Peña C., Lucas P., Guo Z., Smith L., 2024, *MNRAS*, in press

De K. et al., 2023, *Nature*, 617, 55

Dias W. S., Monteiro H., Moitinho A., Lépine J. R. D., Carraro G., Paurzen E., Alessi B., Vilella L., 2021, *MNRAS*, 504, 356

Drew J. E. et al., 2014, *MNRAS*, 440, 2036

Elbakyan V. G., Nayakshin S., Vorobyov E. I., Caratti o Garatti A., Eislöffel J., 2021, *A&A*, 651, L3

Fischer W. J., Hillenbrand L. A., Herczeg G. J., Johnstone D., Kóspál Á., Dunham M. M., 2022, in Inutsuka S., Aikawa Y., Muto T., Tomida K., Tamura M., eds, ASP Conf. Ser. Vol. 534, Protostars and Planets VII. Astron. Soc. Pac., San Francisco, p. 355

Freudling W., Romaniello M., Bramich D. M., Ballester P., Forchi V., García-Dabó C. E., Moehler S., Neeser M. J., 2013, *A&A*, 559, A96

Gagne J., Lambrides E., Faherty J. K., Simcoe R., 2015, *FireHose v2: Firehose v2.0*

Gaia Collaboration, 2016, *A&A*, 595, A2

Gaia Collaboration, 2023, *A&A*, 674, A1

Gullbring E., Hartmann L., Briceño C., Calvet N., 1998, *ApJ*, 492, 323

Guo Z. et al., 2018, *ApJ*, 852, 56

Guo Z. et al., 2020, *MNRAS*, 492, 294

Guo Z. et al., 2021, *MNRAS*, 504, 830

Hackstein M. et al., 2015, *A&A*, 582, L12

Hartmann L., Kenyon S. J., 1996, *ARA&A*, 34, 207

Herbig G. H., 1977, *ApJ*, 217, 693

Herbig G. H., 2007, *AJ*, 133, 2679

Hillenbrand L. A. et al., 2018, *ApJ*, 869, 146

Hillenbrand L. A. et al., 2019, *ApJ*, 874, 82

Hillenbrand L. A. et al., 2021, *AJ*, 161, 220

Hillenbrand L. A., Carvalho A., van Roestel J., De K., 2023, *ApJ*, 958, L27

Hillenbrand L. A., Findeisen K. P., 2015, *ApJ*, 808, 68

Karambelkar V. R. et al., 2023, *ApJ*, 948, 137

Kausch W. et al., 2015, *A&A*, 576, A78

Kopatskaya E. N., Kolotilov E. A., Arkharov A. A., 2013, *MNRAS*, 434, 38

Kóspál Á. et al., 2021, *ApJS*, 256, 30

Kratter K., Lodato G., 2016, *ARA&A*, 54, 271

Lada C. J., 1987, in Peimbert M., Jugaku J., eds, IAU Symp. Vol. 115, Star formation: from OB associations to Protostars. IAU Symposium, p. 1

Lang D., 2014, *AJ*, 147, 108

Lin D. N. C., Papaloizou J., Faulkner J., 1985, *MNRAS*, 212, 105

Liu H. et al., 2022, *ApJ*, 936, 152

Lodato G., Clarke C. J., 2004, *MNRAS*, 353, 841

Lucas, P. et al. 2024, *MNRAS*,

Mainzer A. et al., 2014, *ApJ*, 792, 30

Meisner A. M., Lang D., Schlegel D. J., 2017, *AJ*, 153, 38

Meyer M. R., Calvet N., Hillenbrand L. A., 1997, *AJ*, 114, 288

Minniti D. et al., 2010, *New Astron.*, 15, 433

Minniti D., 2016, in Galactic Surveys: New Results on Formation, Evolution, Structure and Chemical Evolution of the Milky Way. Galactic Surveys, Sesto (BZ) Italy, p. 10

Moorwood A., Cuby J. G., Lidman C., 1998, *The Messenger*, 91, 9

Nayakshin S., Elbakyan V., 2023, preprint ([arXiv:2309.12072](https://arxiv.org/abs/2309.12072))

Nayakshin S., Owen J. E., Elbakyan V., 2023, *MNRAS*, 523, 385

Park S. et al., 2020, *ApJ*, 900, 36

Planck Collaboration, 2016, *A&A*, 594, A28

Saito R. K. et al., 2012, *A&A*, 537, A107

Scholz A., 2012, *MNRAS*, 420, 1495

Simcoe R. A. et al., 2013, *PASP*, 125, 270

Siwak M. et al., 2023, *MNRAS*, 524, 5548

- Smette A. et al., 2015, *A&A*, 576, A77
Smith L. C. et al., 2018, *MNRAS*, 474, 1826
Stetson P. B., 1987, *PASP*, 99, 191
Szabó Z. M. et al., 2021, *ApJ*, 917, 80
Szabó Z. M. et al., 2022, *ApJ*, 936, 64
Szegedi-Elek E. et al., 2020, *ApJ*, 899, 130
Tonry J. L. et al., 2018, *PASP*, 130, 064505
Tylenda R. et al., 2011, *A&A*, 528, A114
Vernet J. et al., 2011, *A&A*, 536, A105
Vorobyov E. I., Basu S., 2015, *ApJ*, 805, 115
Vorobyov E. I., Elbakyan V. G., Liu H. B., Takami M., 2021, *A&A*, 647, A44
Wang S., Chen X., 2019, *ApJ*, 877, 116
Wright E. L. et al., 2010, *AJ*, 140, 1868
Zhu Z., Espaillat C., Hinkle K., Hernandez J., Hartmann L., Calvet N., 2009a, *ApJ*, 694, L64

- Zhu Z., Hartmann L., Gammie C., 2009b, *ApJ*, 694, 1045

SUPPORTING INFORMATION

Supplementary data are available at *MNRASL* online.

suppl_data

Please note: Oxford University Press is not responsible for the content or functionality of any supporting materials supplied by the authors. Any queries (other than missing material) should be directed to the corresponding author for the article.

This paper has been typeset from a \TeX/L\AA\TeX file prepared by the author.